



Research paper

Immune-infiltration based signature as a novel prognostic biomarker in gastrointestinal stromal tumour



Zhe-Wei Wei^{a,†}, Jing Wu^{a,b,†}, Wei-Bin Huang^{a,†}, Jin Li^{a,b,†}, Xiao-Fang Lu^c, Yu-Jie Yuan^a, Wen-Jun Xiong^d, Xin-Hua Zhang^a, Wei Wang^d, Yu-Long He^{a,b,*}, Chang-Hua Zhang^{b,*}

^a Department of Gastrointestinal Surgery, The First Affiliated Hospital of Sun Yat-sen University, 58 Zhongshan 2nd Road, Guangzhou, Guangdong 510080, China

^b Center of Digestive Diseases, The Seventh Affiliated Hospital of Sun Yat-sen University, 628 Zhenyuan Road, Shenzhen, Guangdong 518000, China

^c Department of Pathology, The Seventh Affiliated Hospital of Sun Yat-sen University, 628 Zhenyuan Road, Shenzhen, Guangdong 518000, China

^d Department of Gastrointestinal Surgery, The Second Affiliated Hospital of Guangzhou University of Chinese Medicine, 111 Dade Road, Guangzhou, Guangdong 510120, China

ARTICLE INFO

Article History:

Received 17 February 2020

Revised 3 June 2020

Accepted 4 June 2020

Available online xxx

Keywords:

Gastrointestinal stromal tumours

Tumour-infiltrating lymphocytes

Prognostic biomarker

Immunoscore

Prognosis

ABSTRACT

Background: Accumulating evidence indicates that tumour-infiltrating lymphocytes (TILs) are the primary determinant of survival outcomes in various tumours. Thus, we sought to investigate the TIL distribution and density in gastrointestinal stromal tumours (GISTs) and to develop an immune infiltration (II)-based signature to predict prognosis.

Methods: The expression of 8 immune features in the tumour centre (TC) and tumour margin (TM) and PD-L1 in 435 GIST patients was investigated by immunohistochemistry. Then, a 4-feature-based II-GIST signature integrating the CD3⁺ TC, CD3⁺ TM, CD8⁺ TM and CD45RO⁺ TM parameters was developed using a LASSO Cox regression model in the training cohort and was validated in two separate validation cohorts.

Findings: High CD3⁺ TC, CD3⁺ TM, CD8⁺ TC, CD8⁺ TM, CD45RO⁺ TM, NKp46⁺ TM and CD20⁺ TM correlated with improved survival. Patients with high II-GIST scores have better RFS and OS outcomes than those with low II-GIST scores. Multivariable analyses demonstrated that the II-GIST signature is an independent prognostic factor. The receiver operating characteristic (ROC) curve demonstrated that the prognostic accuracy of the II-GIST signature is superior to that of the NIH risk criteria. Further analysis showed that moderate- and high-risk GIST patients with high II-GIST scores could gain survival benefits from adjuvant imatinib therapy.

Interpretation: The novel II-GIST signature accurately predicted the survival outcomes of GIST patients. In addition, the II-GIST signature was a useful predictor of survival benefit from imatinib therapy amongst moderate- and high-risk patients with GIST.

Funding: This project was supported by National Natural Science Foundation of China (81702325), Natural Science Foundation of Guangdong Province (2017A030310565), and 3&3 Project of the First Affiliated Hospital of Sun Yat-sen University.

© 2020 The Author(s). Published by Elsevier B.V. This is an open access article under the CC BY-NC-ND license. (<http://creativecommons.org/licenses/by-nc-nd/4.0/>)

1. Introduction

Gastrointestinal stromal tumours (GISTs), first proposed by Mazur in 1983, have often been diagnosed as smooth muscle tumours or schwannomas due to the incomplete understanding of their origin and differentiation [1, 2]. With the development of molecular

diagnostic approaches, GISTs have become the most frequently diagnosed mesenchymal malignancy of the gastrointestinal (GI) tract [3]. The US National Institutes of Health (NIH) risk criteria, the most commonly used staging system for GISTs, provide useful but insufficient information to predict prognosis. Therefore, interest in identifying new parameters to improve the predictive accuracy of the current GIST staging system is increasing.

Emerging evidence suggests that immune systems interact with tumour cells and crucially influence multiple tumour processes, such as progression and metastasis [4]. Recent reports have demonstrated that infiltration of immune cells, especially lymphocytes, is critically important in tumours and is a primary determinant of survival outcomes in various types of cancers, including colon, ovarian, lung, gastric and breast cancers [5–8]. There has been considerable progress in

Grants: Supported by National Natural Science Foundation of China, No. 81702325; Natural Science Foundation of Guangdong Province, No. 2017A030310565; 3&3 Project of the First Affiliated Hospital of Sun Yat-sen University.

* Corresponding authors.

E-mail addresses: heyulong@mail.sysu.edu.cn (Y.-L. He),

zhchangh@mail.sysu.edu.cn (C.-H. Zhang).

† ZW Wei, J Wu, WB Huang and J Li contributed equal to this work.

<https://doi.org/10.1016/j.ebiom.2020.102850>

2352-3964/© 2020 The Author(s). Published by Elsevier B.V. This is an open access article under the CC BY-NC-ND license. (<http://creativecommons.org/licenses/by-nc-nd/4.0/>)

Research in context

Evidence before this study

Mounting evidence demonstrated that immune systems interact with tumour cells and crucially influence multiple tumour processes. Tumour-infiltrating lymphocytes (TILs) have been demonstrated to reflect tumour inflammation and to correlate with prognostic outcomes in tumours. We searched PubMed for studies published in English reporting the prognostic effect of tumour-infiltrating lymphocytes in GISTs. The following terms were used as search terms: “gastrointestinal stromal tumors” or “GISTs”, “tumour-infiltrating lymphocytes” or “lymphocytes”. Twelve studies were identified. TILs were reported to be important in GISTs, but the prognostic role has not yet been clearly elucidated

Added value of this study

The prognostic discrimination capability of the II-GIST signature, integrating the CD3⁺ TC, CD3⁺ TM, CD8⁺ TM and CD45RO⁺ TM, was significantly superior to that of the NIH risk criteria. Moderate- and high-risk patients with high II-GIST scores might obtain a greater survival benefit from postoperative imatinib therapy compared with those with low II-GIST scores.

Implications of all the available evidence

The current study indicated that the II-GIST signature based on immune infiltrations can effectively individualize prognostic predictions for GIST patients and serve as a useful predictor of the response to imatinib. Identifying and understanding additional immune abnormalities in GISTs may offer significant implications for future risk stratification and therapeutic opportunities.

Considering the complexity of immune components, individual evaluation of each type of TILs might show only moderate predictive accuracy. Thus, an immune signature comprising multiple types of TILs might notably increase the precision of prognostic estimates. For instance, an immunoscore summarizing the distribution of CD3⁺ and CD8⁺TIL effectors in both the centre and invasive margin of the tumour has been demonstrated to be a reliable model for discriminating prognostic outcomes in colorectal cancer [7]. A recent study demonstrated that a 5-feature-based immunoscore signature was efficacious enough to estimate recurrence risk and predict chemosensitivity in gastric cancer [5]. Thus, we sought to investigate the distribution and density of TILs and to develop an immune infiltration (II)-based signature to predict prognosis and the efficacy of adjuvant imatinib therapy in patients with GIST.

2. Methods

2.1. Ethics statement

This study was approved by the Ethical Review Committee of the First Affiliated Hospital of Sun Yat-sen University and the Second Affiliated Hospital of Guangzhou University of Chinese Medicine. All patients in this study signed an informed consent form.

2.2. Patients and tissue samples

We retrospectively retrieved GIST patient information from the prospectively established database at the First Affiliated Hospital of Sun Yat-sen University and the Second Affiliated Hospital of Guangzhou University of Chinese Medicine. The inclusion criteria were as follows: (1) histologically proven GIST; (2) available archived samples with tumour components and margins; (3) lack of preoperative systemic treatment; (4) absence of synchronous or metachronous cancers; and (5) complete clinicopathological and follow-up information. Finally, 435 eligible formalin-fixed paraffin-embedded specimens that were collected between 2005 and 2015 were used for the current study. We randomly assigned GIST patients from the First Affiliated Hospital of Sun Yat-sen University to the training ($n = 130$) and internal validation ($n = 194$) cohorts. Another 111 patients from the Second Affiliated Hospital of Guangzhou University of Chinese Medicine were enrolled into the external validation cohort. Moderate-risk and high-risk patients who received imatinib were previously analysed for mutations and were identified as having sensitive mutations according to the guidelines [19].

2.3. Assessment of TILs, PD-1 and PD-L1

IHC was performed as previously described [20]. Briefly, tissue sections (4–5 μm in thickness) were deparaffinized and rehydrated. Tissue slides were subjected to antigen retrieval by microwave heating in 10 mM citrate buffer (pH 6.0) and were quickly immersed in 3% H₂O₂ to quench endogenous peroxidase activity. Then, sections were incubated with primary antibodies against CD3 (Ventana, 790–4341; ready-to-use), CD8 (Dako, M7103; 1:100 dilution), CD45RO (Origene, TA807197; 1:100 dilution), CD4 (Abcam, ab213215; 1:300 dilution), Foxp3 (Abcam, ab22510; 1:200 dilution), NKp46 (Abcam, ab214468; 1:500 dilution), CD20 (Abcam, ab27093; 1:200 dilution), programmed death-1(PD-1) (Cell signaling Technology, 43,248; 1:50 dilution), and programmed death-ligand 1 (PD-L1) (Dako, M3653; 1:50 dilution) at 4 °C overnight.

The density and distribution of CD3⁺, CD8⁺, CD45RO⁺, Foxp3⁺, CD4⁺, NKp46⁺, CD20⁺ and PD-1⁺TILs in the samples were assessed in two specific areas: the tumour centre (TC) and tumour margin (TM). The TM is defined as a region 800 μm wide centred on the border of the malignant cells with the fibrous trabeculae, and the TC is defined as the central tumour tissue surrounded by the TM (Fig. S1). Two

understanding the role of patients' pre-existing tumour-specific immunity—especially that related to tumour-infiltrating lymphocytes (TILs), which act as prognostic biomarkers in tumour progression [9, 10]. Tumour levels of CD3⁺lymphocytes have been demonstrated to be independent prognostic indicators [11]. CD8⁺cytotoxic T lymphocytes (CTLs), key components of the immune system, can potentially target and eliminate tumour cells and are correlated with favourable survival outcomes [12]. CD45, a transmembrane phosphatase, regulates cytokine signalling and various corresponding biological processes, including cell proliferation, differentiation and activation [13]. Accumulating evidence suggests that patients with tumours that have high CD45RO⁺ T cell densities have less tumour invasiveness and better survival outcomes [14]. A meta-analysis performed in breast cancer demonstrated that TILs are predictors of a favourable response to chemotherapy [15]. With respect to GISTs, Rusakiewicz et al. demonstrated that infiltrations of CD3⁺ and NKp46⁺ cells are associated with a reduced relapse rate in the 54 GIST patients using immunohistochemistry (IHC) [16]. Vitiello et al. indicated that compared with KIT-mutant GIST, the infiltrations of CD45RO⁺ and CD8⁺ cells are higher in PDGFRA-mutant GISTs by IHC, which comparatively tend to be resistant to imatinib [17]. Balachandran et al. reported that inhibition of oncogenic KIT in tumour cells promoted the apoptosis of regulatory Foxp3⁺ T cells and CD4⁺ TILs are diffusely infiltrated in GISTs [18]. However, the prognostic role of these TILs has not yet been clearly elucidated. Although seldom reported in GIST, CD20 expressing on the surface of all B-cells, which are an important type of lymphocyte, has also been selected as a B-lymphocyte antigen. Hence, the current study sought to investigate the prognostic impact of CD3⁺, CD8⁺, CD45RO⁺, Foxp3⁺, CD4⁺, NKp46⁺ and CD20⁺ TILs in GISTs.

pathologists (Lu XF and Ding L), who were blinded to the clinicopathological features, reviewed the stained slides to determine the TC and TM regions. Each pathologist independently selected 5 high-power fields (at $200 \times$ magnification) in each region to assess the density of stained immune cells. ImageJ was used to calculate the absolute counts of TILs according to the operating parameters established by the two pathologists [21]. If scores were obviously different or if the infiltration was heterogeneous, the two pathologists worked collaboratively to provide a result. If major discrepancies still existed, a third pathologist (Professor Xue L) assessed the samples and collaborated with the other two to provide a final result. The cases of major discrepancy between the two pathologists in review were 188 (2.4%). The optimum density threshold for each feature was determined with the R package “Maxstat,” as previously described [22].

Staining intensity of PD-L1 was graded as negative, weak, moderate, or strong. Samples with 10% of tumour cells exhibiting moderate to strong staining intensity for PD-L1 were deemed as positive.

2.4. Construction of the II-based signature

Considering the comparatively limited number of events in the training cohort relative to the number of variables and avoiding over-fitting due to the high dimensionality of the immune-infiltration-based signature, the least absolute shrinkage and selection operator (LASSO) was utilized to select significant features and obtain an optimal model. LASSO is a robust method that can be used with high-dimensional data for optimal selection of factors with strong diagnostic or prognostic value [23, 24]. LASSO shrinks the absolute size of coefficient estimates towards exactly zero depending on a penalized factor called λ , and thereby minimizes the prediction error. Briefly, as the value of λ increases, the coefficients of predictors in LASSO decrease (even to zero), which is pivotal for the establishment of a low-dimensional model with interpretability. In order to avoid over-fitting, 10-time cross-validation was used to determine the coefficients of LASSO modelling. Meanwhile, the mean-squared error should be as small as possible to improve the prediction accuracy. If λ with minimal partial likelihood deviance was used, 10 features would be chosen, which might lead to over-fitting. Hence, 1-SE criteria was used to select lambda ($\lambda=0.0634$) for further analysis. Here, a value $\lambda=0.0634$ with $\log(\lambda)=-2.759$ was determined by 10-time cross-validation via 1-SE criteria in our study. Four parameters ($CD3^+$ TC, $CD3^+$ TM, $CD8^+$ TM and $CD45RO^+$ TM) were finally included in the II-based signature in the training cohort (Fig. 1). The II-GIST score was calculated as follows: $(0.0000019123 \times CD3^+$ TC count) + $(0.0000559617 \times CD3^+$ TM count) + $(0.0028924318 \times CD8^+$ TM

count) + $(0.0007187206 \times CD45RO^+$ TM count). The R package “glmnet” was used for the LASSO Cox regression analysis [25]. We used maximally selected rank statistics to define the threshold value for II-GIST as 0.58 in order to divide patients into the high II-GIST and low II-GIST groups. According to the above formula, high expression was defined as 1, and low expression was defined as 0.

2.5. Statistical analysis

For categorical variables, the associations between the TIL densities and the clinicopathological features were analysed via the χ^2 test or Fisher’s exact test. For continuous variables, parametric or non-parametric tests were used to compare the differences between groups.

Survival curves were calculated by the Kaplan-Meier method and were compared by log-rank tests. We conducted univariate analysis to investigate the associations between clinicopathological features and survival outcomes. Variables with $P < 0.25$ in the univariate analysis were incorporated into a multivariable analysis that employed a Cox proportional hazards model using the backward method. The Cox model was also used to investigate the interactions between the II-GIST signature and adjuvant imatinib therapy. The time-dependant area under the receiver operating characteristic (ROC) curve (AUC) was calculated to compare the prognostic discrimination capability of each immune infiltration and the prediction models for GISTs. In addition, Harrell’s concordance index (C-index) with 95% confidence interval (CI) was calculated to evaluate discrimination by the II-GIST signature and the NIH risk criteria. The relative importance of each parameter to survival risk was assessed using the χ^2 statistics by R package “rms” [26]. All statistical analyses were performed with SPSS (Inc., Chicago, IL, USA) and R software.

3. Results

3.1. Density and distribution of TILs in GISTs

Initially, $CD3^+$, $CD8^+$, $CD45RO^+$, $Foxp3^+$, $CD4^+$, $NKp46^+$ and $CD20^+$ cells were evaluated separately in the TC and TM (Fig. S2). More $CD3^+$, $CD8^+$, $CD4^+$ and $NKp46^+$ cells were detected in the TM than in the TC (Fig. S3a, b, e and f). The densities of $CD45RO^+$, $Foxp3^+$ and $CD20^+$ cells were similar between the TC and TM (Fig. S3c, d and g).

Then, we analysed the associations between the clinicopathological variables and the absolute counts of $CD3^+$, $CD8^+$, $CD45RO^+$, $Foxp3^+$, $CD4^+$, $NKp46^+$ and $CD20^+$ cells in the TC and TM. Localized GISTs exhibited higher $CD8^+$ (Wilcoxon Rank Sum test, $P = 0.008$) and $Foxp3^+$ (Wilcoxon Rank Sum test, $P < 0.001$) cell densities in the TM compared with metastatic GISTs (Fig. S4b and d). The $CD45RO^+$ cell counts in the TC were higher in tumours ≤ 5 cm in size than in tumours > 5 cm in size (Wilcoxon Rank Sum test, $P = 0.023$) (Fig. S5c). Stomach GISTs exhibited a lower prevalence of $CD8^+$ cells in both the TC (Wilcoxon Rank Sum test, $P = 0.001$) and TM (Wilcoxon Rank Sum test, $P = 0.001$) than non-gastric GISTs (Fig. S6b).

Next, we investigated associations between the density of TILs in the TC or TM and the prognosis of GIST patients. The Kaplan-Meier analysis results suggested that high levels of $CD3^+$, $CD8^+$, $CD45RO^+$, $NKp46^+$ and $CD20^+$ cell infiltration in both the TC and TM correlated with improved recurrence-free survival (RFS) and overall survival (OS) outcomes (Fig. 2 and Fig. S7–9). The time-dependant ROC curve analysis revealed the prognostic discrimination capability of individual TILs (Fig. S10 and Table S1–2). Multivariable Cox proportional regression analyses after adjustment for other clinicopathological variables demonstrated that high levels of $CD3^+$ TC, $CD3^+$ TM, $CD8^+$ TC, $CD8^+$ TM, $CD45RO^+$ TM, $NKp46^+$ TM and $CD20^+$ TM infiltrations were independent prognostic factors for GIST outcomes (Table S3). In addition, moderate correlations were detected in pairs (TC and TM)

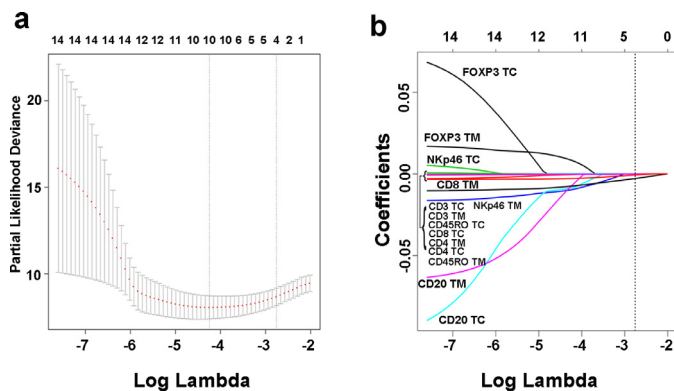


Fig. 1. Construction of the II-GIST signature comprising 4 immune features. (a) Tenfold cross validation for tuning parameter selection in the LASSO model. The solid vertical lines represent partial likelihood deviance \pm standard error (SE) values. The dotted vertical lines are drawn at the optimal values according to the minimum criteria and 1-SE criteria. Here, a value of $\lambda=0.0634$ with $\log(\lambda)=-2.759$ was selected by 10-fold cross validation with the 1-SE criteria. (b) LASSO coefficient profiles of the GIST-associated immune features.

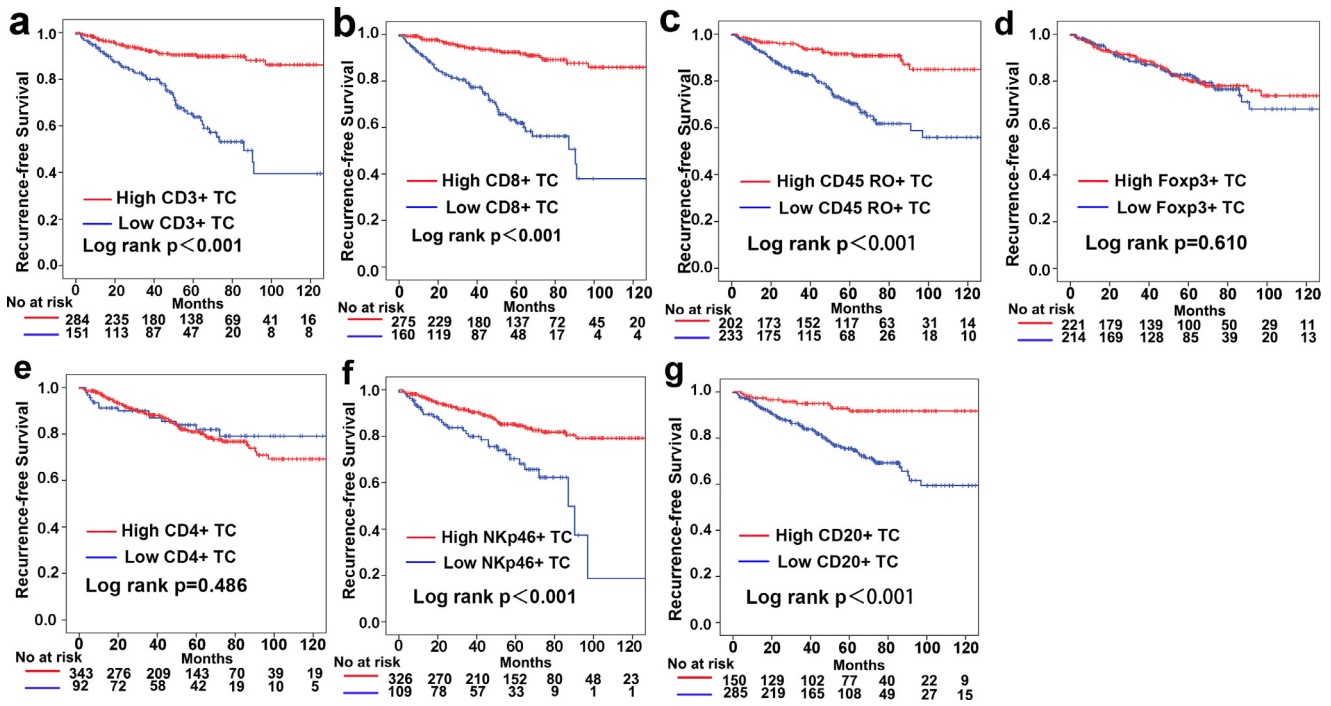


Fig. 2. Kaplan-Meier analysis of RFS according to individual TIL populations in the TC. (a) CD3⁺ TC. (b) CD8⁺ TC. (c) CD45RO⁺ TC. (d) Foxp3⁺ TC. (e) CD4⁺ TC. (f) NKp46⁺ TC. (g) CD20⁺ TC.

of CD3⁺, CD8⁺, CD45RO⁺, CD20⁺ and NKp46⁺ TILs, as shown in Figure S11.

3.2. II-GIST signature and survival of GIST patients

The baseline characteristics of the training, internal validation and external validation cohorts are listed in Table 1. First, we developed a prediction model using a LASSO Cox regression model based on the training cohort, which ultimately included 4 immune features (Fig. 1).

As shown in Table 1, the baseline clinicopathological features were similar between the high II-GIST and low II-GIST groups in both the training and internal validation cohorts, while in the external validation cohort, the low II-GIST group seemed to have more advanced

disease characteristics. In the training cohort, 77 patients were classified into the high II-GIST group, and 53 were assigned to the low II-GIST group. In the training cohort, the 5-year RFS and OS rates were 94.1 and 94.8%, respectively, in the high II-GIST group and 52.6 and 57.2%, respectively, in the low II-GIST group (Fig. 3a). In the internal validation cohort, the RFS (HR=0.110; 95% CI, 0.044–0.274; $P<0.001$) and OS (HR=0.162; 95% CI, 0.061–0.426; $P<0.001$) rates in the high II-GIST group were significantly superior to those in the low II-GIST group (Fig. 3b). Similarly, the high II-GIST group exhibited higher RFS and OS rates than the low II-GIST group in the external validation cohort (Fig. 3c). Multivariable Cox regression analyses demonstrated that II-GIST was an independent prognostic factor for both RFS and OS (Table S4–7).

Table 1

Clinical characteristics of patients according to the II-GIST Signature in the training and validation cohorts.

| | Training Cohort (n = 130) | | | | Internal Validation Cohort (n = 194) | | | | External Validation Cohort (n = 111) | | | |
|---------------------|---------------------------|--------------|-------------|-------|--------------------------------------|--------------|-------------|-------|--------------------------------------|--------------|-------------|-------|
| | n | High-II-GIST | Low-II-GIST | P | n | High-II-GIST | Low-II-GIST | P | n | High II-GIST | Low II-GIST | P |
| Median age (range) | | 56 (23–77) | 56 (27–80) | 0.542 | | 56 (26–94) | 59 (28–76) | 0.934 | | 60 (27–83) | 61 (44–87) | 0.070 |
| Sex | | | | 0.229 | | | | 0.707 | | | | 0.803 |
| Male | 72 | 46 | 26 | | 120 | 73 | 47 | | 45 | 29 | 16 | |
| female | 58 | 31 | 27 | | 74 | 43 | 31 | | 66 | 41 | 25 | |
| tumour size | | | | 0.607 | | | | 0.154 | | | | 0.176 |
| ≤5cm | 75 | 43 | 32 | | 109 | 70 | 39 | | 66 | 45 | 21 | |
| >5cm | 55 | 34 | 21 | | 85 | 46 | 39 | | 45 | 25 | 20 | |
| Primary tumour site | | | | 0.369 | | | | 0.152 | | | | 0.901 |
| Stomach | 82 | 51 | 31 | | 120 | 67 | 53 | | 75 | 47 | 28 | |
| Non-Stomach | 48 | 26 | 22 | | 74 | 49 | 25 | | 36 | 23 | 13 | |
| Mitotic index | | | | 0.202 | | | | 0.251 | | | | 0.041 |
| ≤5 | 96 | 60 | 36 | | 131 | 82 | 49 | | 85 | 58 | 27 | |
| >5 | 34 | 17 | 17 | | 63 | 34 | 29 | | 26 | 12 | 14 | |
| NIH criteria | | | | 0.055 | | | | 0.165 | | | | 0.036 |
| High risk | 54 | 26 | 28 | | 90 | 48 | 42 | | 33 | 15 | 18 | |
| Intermediate risk | 31 | 23 | 8 | | 32 | 19 | 13 | | 21 | 16 | 5 | |
| Very Low/Low risk | 45 | 28 | 17 | | 72 | 49 | 23 | | 57 | 39 | 18 | |
| Imatinib therapy | | | | 0.478 | | | | 0.362 | | | | 0.264 |
| Yes | 18 | 12 | 6 | | 20 | 10 | 10 | | 31 | 17 | 14 | |
| No | 112 | 65 | 47 | | 174 | 106 | 69 | | 80 | 53 | 27 | |

Abbreviation: II, Immune-infiltration (II) based Signature; NIH, National Institutes of Health. Mitotic index, mitoses/50 high-power field;.

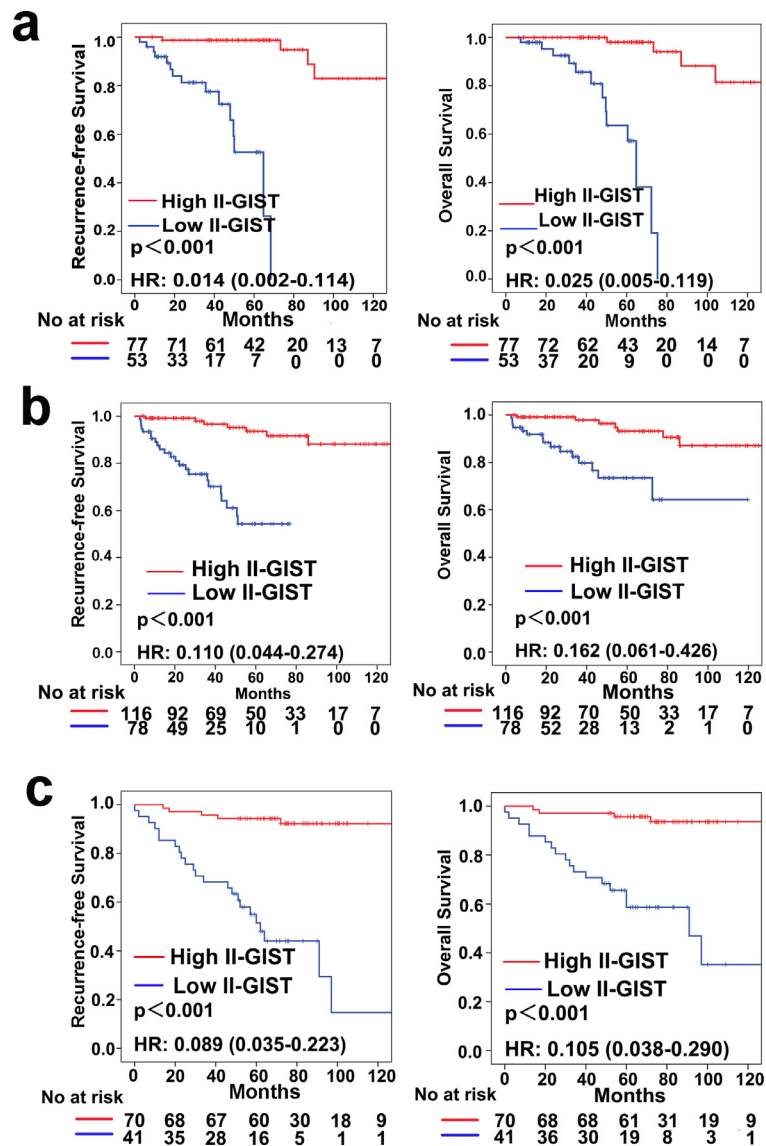


Fig. 3. Prognostic impact of the II-GIST signature on RFS and OS. Kaplan-Meier curves of RFS and OS according to the II-GIST signature in the (a) training cohort, (b) internal validation cohort, and (c) external validation cohort. Left panel: RFS; Right panel: OS.

To explore the prognostic discrimination capability of the II-based signature in GIST patients, we performed a time-dependent ROC curve analysis. The AUC values for RFS at 1, 3 and 5 years were 0.81 (95% CI: 0.66–0.96), 0.91 (95% CI: 0.84–0.97) and 0.92 (95% CI: 0.86–0.99), respectively, in the training cohort and 0.87 (95% CI: 0.80–0.95), 0.87 (95% CI: 0.80–0.95) and 0.91 (95% CI: 0.83–0.98), respectively, in the internal validation cohort. The AUC values for RFS at 1, 3 and 5 years were 0.82 (95% CI: 0.71–0.92), 0.81 (95% CI: 0.72–0.90) and 0.88 (95% CI: 0.81–0.95), respectively, in the external validation cohort (Fig. S12). ROC curve analysis suggested that the II-GIST signature is potentially more accurate than the NIH risk criteria in terms of prognostic prediction in the internal and external validation cohorts (Fig. 4a–d). In addition, the concordance index for the II-GIST signature was 0.842 (95% CI: 0.800–0.885) in the internal cohort and 0.821 (95% CI: 0.757–0.883) in the external cohort and was superior to the concordance index for the NIH criteria, at 0.677 (95% CI 0.600–0.755) in the internal cohort and 0.640 (95% CI 0.526–0.739) in the external cohort (Table S8). The χ^2 test of proportions demonstrated that the risk in GIST patients is determined mostly by the II-GIST signature (92.3% in the internal validation cohort; 90.5% in the external validation cohort) compared with other features, such as the

NIH risk criteria (7.5% in the internal validation cohort; 7.1% in the external validation cohort) and tumour size (0.2% in the internal validation cohort; 2.4% in the external validation cohort) (Fig. 4e–f).

Furthermore, subgroup analyses stratified by clinicopathological features were performed to explore the ability of the II-GIST signature to predict the prognosis of GIST patients in the internal and external validation cohorts. High II-GIST patients showed better OS and RFS outcomes than both low II-GIST patients with moderate/high risk and GIST patients with very low/low risk (Fig. 5). When the cohorts were stratified by tumour size, mitotic index and primary tumour location, the II-GIST signature remained an efficient prognostic model (Fig. S13–15).

3.3. II-GIST signature and the benefit of adjuvant imatinib therapy

Current clinical practice recommends adjuvant imatinib therapy after surgery for moderate- and high-risk patients with GIST. Thus, the association between the II-GIST signature and the benefit of imatinib treatment was explored amongst moderate- and high-risk groups of patients with GISTs. The benefit of adjuvant imatinib therapy in the high II-GIST group was obvious for both RFS (HR=0.134;

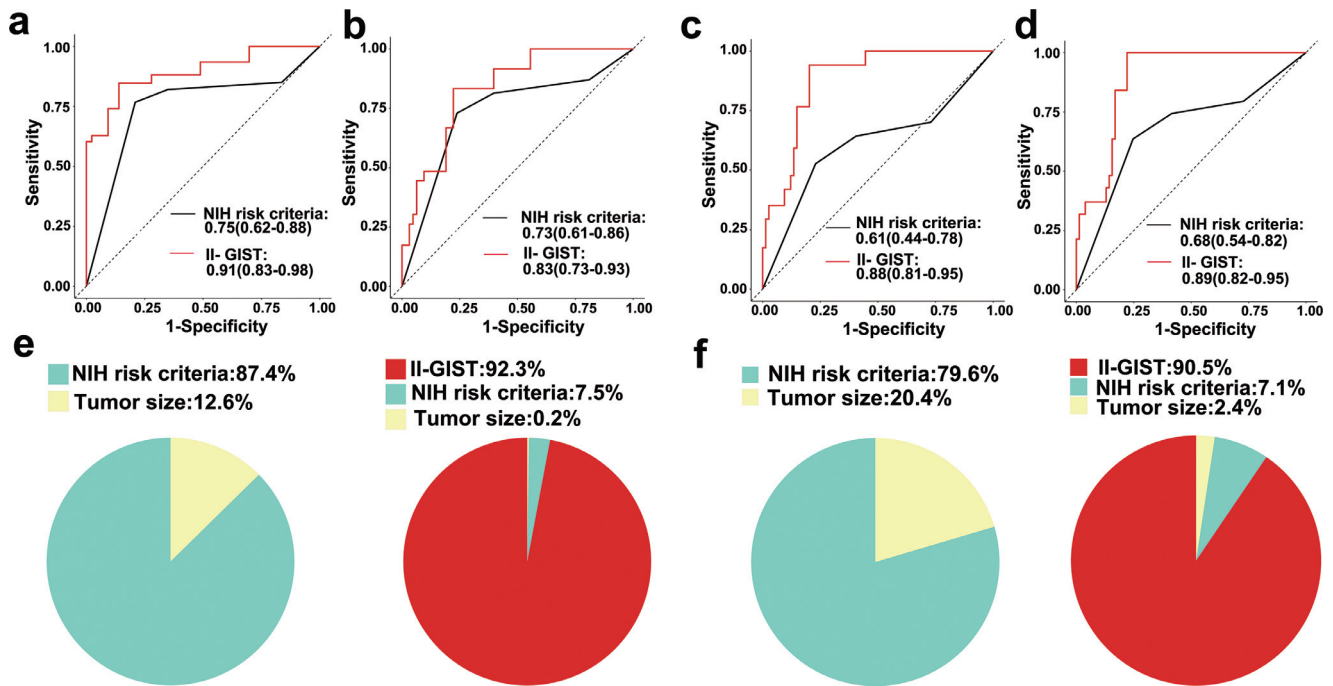


Fig. 4. Prognostic discrimination and relative contribution of the II-GIST signature to the prognosis of GIST patients in the internal and external validation cohorts. Time-dependent ROC curves of II-GIST and NIH risk criteria as predictors of (a) RFS in the internal validation cohort, (b) OS in the internal validation cohort, (c) RFS in the external validation cohort, and (d) OS in the external validation cohort. The relative importance of each risk parameter to survival risk was evaluated using the χ^2 test of proportions for clinical parameters and clinical parameters plus the II-GIST signature in the (e) internal validation cohort and (f) external validation cohort.

95% CI, 0.025–0.724; $P = 0.020$; $P = 0.001$ for the interaction) and OS (HR=0.050; 95% CI, 0.006–0.440; $P = 0.007$; $P = 0.006$ for the interaction) (Table S9). The Kaplan-Meier survival curves revealed that adjuvant imatinib therapy significantly improved RFS (log-rank $P = 0.020$) and OS (log-rank $P = 0.007$) outcomes in the high II-GIST group, although no obvious differences were detected in the low II-GIST group (Fig. 6). Taken together, our data suggest that moderate- and

high-risk patients with high II-GIST scores may gain survival benefits from adjuvant imatinib therapy.

3.4. PD-1 and PD-L1 in GISTs

Moreover, we analysed the expression of PD-1 and PD-L1 in GIST patients in the whole cohort (Fig. S16–17). The densities of PD-

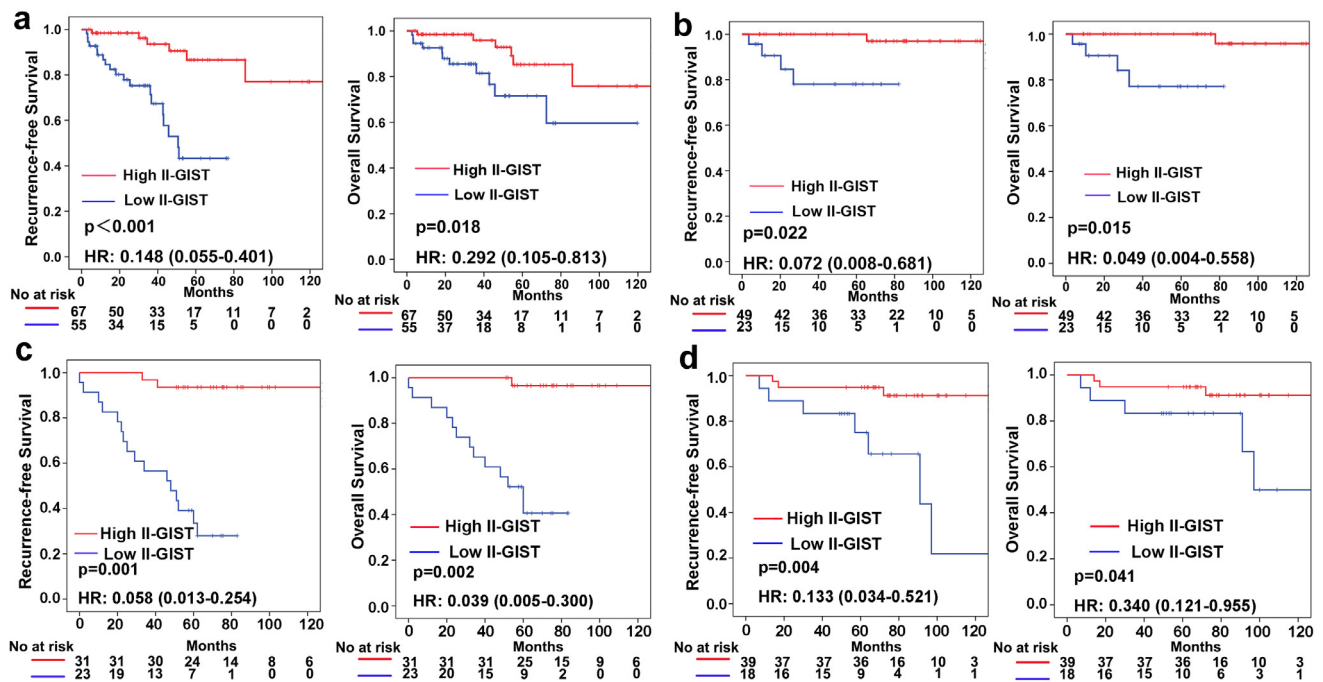


Fig. 5. Kaplan-Meier survival analysis of RFS and OS according to the II-GIST signature in the internal and external validation cohorts stratified by NIH risk criteria (moderate/high and very low/low risk). (a) NIH moderate- and high-risk GISTs in the internal validation cohort. (b) NIH very low- and low-risk GISTs in the internal validation cohort. (c) NIH moderate- and high-risk GISTs in the external validation cohort. (d) NIH very low- and low-risk GISTs in the external validation cohort. Left panel: RFS; Right panel: OS.

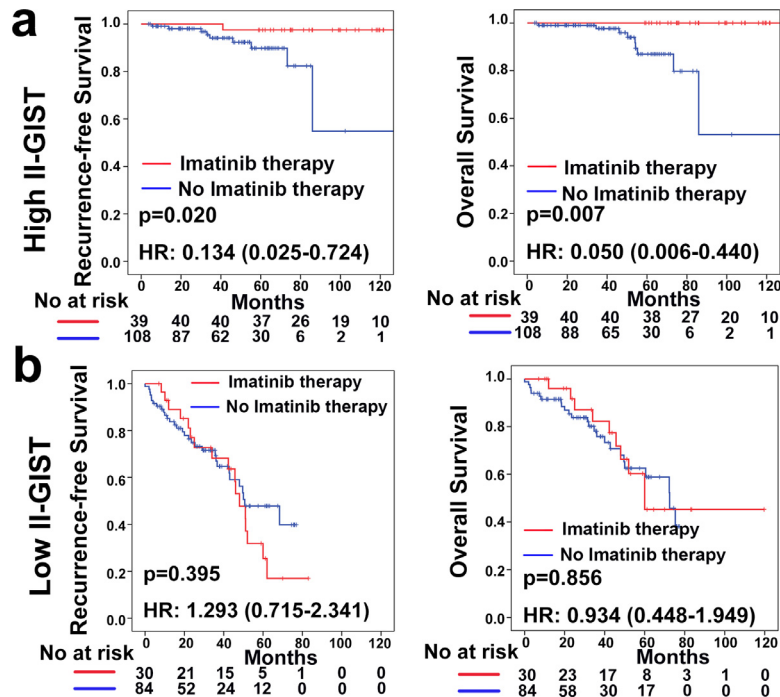


Fig. 6. Association between the II-GIST signature and survival benefit of imatinib therapy in groups of moderate- and high-risk patients with GIST. (a) Kaplan-Meier analysis of RFS (left panel) and OS (right panel) in the high II-GIST group according to imatinib therapy status. (b) Kaplan-Meier analysis of RFS (left panel) and OS (right panel) in the low II-GIST group according to imatinib therapy status.

1^+ cells were similar between the TC and TM (Fig. S3h). The Kaplan-Meier analysis results indicated that high PD-1 expression in TC or TM are not associated with RFS or OS (Fig. S18a-b). PD-L1 expression was found to be positive in only 75 cases (16.3%). No significant difference of survival outcomes was detected between the PD-L1-positive and -negative group, either (Fig. S18c). Seifert et al. suggested that PD-1/PD-L1 blockade enhance T-cell activity and antitumor efficacy of imatinib in murine GISTs [27]. Then, the correlation between PD-L1 expression and response to imatinib was also evaluated amongst moderate- and high- risk patients. However, the benefit from adjuvant imatinib therapy were not discernable in neither PD-L1 positive nor negative group (Fig. S19).

4. Discussion

The immune microenvironment has attracted intense attention in the past decade because of the astounding progress in immunotherapy [28]. TILs, critical components of the immune microenvironment, participate in a complex interplay with their surroundings through which they influence tumour progression, development and metastasis [29]. During the past several decades, revolutionary progress has occurred in the diagnosis, management and understanding of the molecular mechanisms of GIST, a disease that has been historically consistently misdiagnosed as leiomyoma. However, the role of TILs in GISTs has rarely been addressed. The present study investigated the density and prognostic significance of infiltrating immune cell subpopulations in the TC and TM and proposed an II-based signature to predict prognosis and survival benefits from imatinib therapy.

Over the past decade, TILs have been demonstrated to reflect tumour inflammation and to correlate with prognostic outcomes in tumours [30-32]. The function of TILs, especially $CD8^+$ T cells, is to identify unique tumour antigens and block tumour immune escape via avoidance of immune recognition [33, 34]. The distribution, density and function of various TIL subsets differ in each spatial location of the tumour [35]. Some studies have suggested that infiltration of the TC and TM by TILs may exert varied influences on survival

outcomes in cancers [36-38]. Thus, we investigated the distribution and prognostic impact of separate TIL populations and demonstrated that the $CD8^+$ and $Foxp3^+$ cell densities in the TM are higher in localized tumours than in metastatic tumours. $CD45RO^+$ lymphocytes are memory lymphocytes that are indispensable for host defence [39]. Consistent with a prior report in breast cancer [40], our study showed that high infiltration levels of $CD45RO^+$ cells in the TC is associated with small GIST size.

Accumulating literature indicates that TILs in tumours are efficient predictive indicators of prognosis [33, 41]. Higher infiltration levels of $CD8^+$ CTLs, important components of tumour-specific cellular adaptive immunity, were associated with better prognosis and pathological complete response to chemotherapy [29, 42]. In addition, $CD3^+$ T lymphocytes have been associated with prolonged RFS in hepatocellular carcinoma [12]. $NKp46^+$ NK cells, a population of lymphocytes that are part of the innate immune system, were found to correlate significantly with more favourable survival in gastrointestinal malignancies [43, 44]. Tumour-infiltrating $CD20^+$ B cells ($CD20^+$ TILs) play a vital role and are correlated with increased survival in ovarian cancer [45]. In GISTs, accumulating evidence indicates that several haematologic biomarkers, including the platelet-to-lymphocyte ratio (PLR) and neutrophil-to-lymphocyte ratio (NLR), which are precise predictors of prognosis, should include lymphocytes to reflect immunity and inflammation [46-48]. Regarding TILs, Rusakiewicz et al. reported that $NKp46^+$ and $CD3^+$ cell infiltrates were associated with lower rates of recurrence and smaller tumour sizes amongst 53 localized GISTs [16]. In the present study, we investigated the prognostic impact of each TIL population and suggested that high infiltration levels of $CD3^+$ TC, $CD3^+$ TM, $CD8^+$ TC, $CD8^+$ TM, $CD45RO^+$ TM, $NKp46^+$ TM and $CD20^+$ TM infiltrations are associated with favourable prognosis. Infiltrating immune cells contribute to immunosurveillance, which eliminates tumour cells and slows immune evasion [49, 50]. Convincing evidence indicates that the presence of tumour immune infiltrates is associated with a good response to treatment in different malignancies [35, 42, 51]. The abovementioned mechanisms might

clarify the association between high infiltration levels of TILs and favourable prognoses of patients with GISTs.

Relapse remains a common clinical occurrence even after complete resection of GISTs [52], and precise estimation of the recurrence risk is crucial for the management of GISTs [53]. Currently, the survival outcomes vary amongst GIST patients with identical NIH risk criteria. Due to the inadequate accuracy of the NIH risk criteria, a novel scoring system to evaluate the prognosis of patients with GISTs is urgently needed. The innate immune system performs critical functions in protecting the host from tumours; thus, the focus on immune profiling has increased. TILs have been shown to be positively correlated with the prognosis of patients with various kinds of solid tumours, including GISTs [5, 6, 16, 54]. Historically, the role of TILs has been largely investigated in individual TIL populations despite the complexity of immune features, which has led to the discovery of moderate predictive ability of TIL-related markers. Integrating numerous immune infiltrates into a single model has resulted in improved prognostic performance for individualized recurrence risk in several cancer types [5, 32, 35]. Hence, we developed a novel II-based signature with 4 immune features to independently predict the prognosis of GIST patients. The II-GIST signature is an indicator of bio-immunological characteristics, while the NIH risk criteria are determined mainly according to the following pathologic parameters: tumour size, mitotic index, nuclear pleomorphism, and tumour necrosis [55]. Our data indicated that the prognostic discrimination capability of the II-GIST signature was significantly superior to that of the NIH risk criteria and exhibited the greatest ability to predict survival risk when it was combined with other clinicopathological features into one model. The II-GIST signature is a comprehensive reflection of the immune environment and is correlated with tumour surveillance and progression and exhibited excellent accuracy for prognostic predictions. When patient cohorts were stratified by other clinicopathological parameters, the II-GIST signature still improved the accuracy of prognostic predictions.

Adjuvant imatinib therapy has been recommended as a first-line postoperative treatment for moderate- and high-risk patients with GISTs harbouring sensitive mutations [19]. However, the population of moderate- and high-risk patients with GISTs exhibits considerable heterogeneity, which has led to great difficulties in distinguishing patients who could benefit from imatinib treatment. Emerging evidence suggests that TILs are independent predictors of the chemotherapeutic response of solid tumours. Asano et al. demonstrated that a high CD8⁺/Foxp3⁺ TIL ratio correlates with pathological complete response to neoadjuvant chemotherapy in aggressive breast cancer [51]. Balachandran et al. demonstrated that in GISTs, intratumoural CD3⁺ and CD8⁺ cell infiltration is associated with a favourable response to imatinib [18]. Rusakiewicz et al. reported that the NKp46/Foxp3 ratio in the TC increased significantly after imatinib treatment [16]. Thus, we investigated correlations between the novel II-GIST signature and the benefit of adjuvant imatinib treatment in moderate- and high-risk patients with GISTs. Our data suggested that moderate- and high-risk patients with high II-GIST scores might obtain a greater survival benefit from postoperative imatinib therapy compared with those with low II-GIST scores. Balachandran et al. showed that imatinib amplifies a pre-existing immune response in mouse GIST and that CD8⁺T cells are required for its maximal effects [18]. Borg indicated that imatinib promotes NK cell activation and NK cell-dependant antitumour effects in GISTs [56]. Taken together, lymphocytes contribute substantially to the antitumour effects of imatinib. The II-GIST signature based on TILs is a comprehensive reflection of the immune status of GIST patients, which may correspondingly predict the effect of imatinib in GISTs. Hence, the II-GIST signature may have the potential to serve as a useful predictor of the response to imatinib and offer better guidance than existing indices for clinical selection of patients who can benefit from imatinib therapy. Considering the limited number of patients received imatinib, the predictive

accuracy of the II-GIST signature to imatinib therapy needs to be further validated in larger datasets. Furthermore, Seifert et al. reported that PD-L1 inhibition might augment both the therapeutic effect of imatinib and T cell activity in GISTs [27]. But in the present study the benefit from adjuvant imatinib therapy are not associated with PD-L1 status (Fig. S19). Consequently, application of the II-GIST signature may contribute to treatment optimization, including that of future immunotherapies.

Some limitations of our study need to be addressed. First, this was a retrospective study, and all enrolled patients were of Chinese ethnicity. Second, the sample size seemed to be limited. However, given the comparatively low incidence of GISTs, the current study is one of the largest clinical studies conducted to date. Therefore, the prognostic impact of the II-GIST signature must be validated in further prospective studies to guide clinicians in the identification of patients who require more frequent monitoring and intensive therapy.

5. Conclusion

In conclusion, the novel II-GIST signature can effectively individualize prognostic predictions for GIST patients and improve the predictive accuracy of common clinicopathological indices. Moreover, the II-GIST signature may have the potential to predict the therapeutic response to imatinib in moderate- and high-risk patients with GISTs. Therefore, the II-GIST signature might guide patient counselling, decision-making regarding individualized adjuvant treatment, and follow-up scheduling.

Funding

This study was supported by National Natural Science Foundation of China, No. 81702325; Natural Science Foundation of Guangdong Province, No. 2017A030310565; 3&3 Project of the First Affiliated Hospital of Sun Yat-sen University. The funders had no role in study design, data collection and analysis, decision to publish, or preparation of the manuscript.

Ethics approval and consent to participate

This study was reviewed and approved by the Ethics Committee of the first affiliated hospital of Sun Yat-sen University and the second affiliated hospital of Guangzhou University of Chinese Medicine.

Author contributions

CH Zhang, YL He and ZW Wei contributed to the study design. J Wu, J Li, WJ Xiong, ZW Wei and XF Lu performed immunohistochemistry. WB Huang, W Wang, J Wu and XF Lu performed statistical analysis and interpretation. XH Zhang, J Wu and WB Huang drafted the manuscript. All authors contributed to critical revision of the final manuscript and approved the final version of the manuscript.

Declaration of Competing Interest

The authors declare that they have no conflict of interest.

Acknowledgment

The authors would like to acknowledge the assistance of Donglian Chen in maintaining our database.

Supplementary materials

Supplementary material associated with this article can be found, in the online version, at [doi:10.1016/j.ebiom.2020.102850](https://doi.org/10.1016/j.ebiom.2020.102850).

References

- [1] Mei L, Smith SC, Faber AC, Trent J, Grossman SR, Stratakis CA, et al. Gastrointestinal stromal tumors: the GIST of precision medicine. *Trends Cancer* 2018;4(1):74–91.
- [2] Nishida T, Blay JY, Hirota S, Kitagawa Y, Kang YK. The standard diagnosis, treatment, and follow-up of gastrointestinal stromal tumors based on guidelines. *Gastric Cancer* 2016;19(1):3–14.
- [3] Valsangkar N, Sehdev A, Misra S, Zimmers TA, O'Neil BH, Koniaris LG. Current management of gastrointestinal stromal tumors: surgery, current biomarkers, mutations, and therapy. *Surgery* 2015;158(5):1149–64.
- [4] Yang Y. Cancer immunotherapy: harnessing the immune system to battle cancer. *J Clin Invest* 2015;125(9):3335–7.
- [5] Jiang Y, Zhang Q, Hu Y, Li T, Yu J, Zhao L, et al. ImmunoScore signature: a prognostic and predictive tool in gastric cancer. *Ann Surg* 2018;267(3):504–13.
- [6] Fortis SP, Sofopoulos M, Sotiriadou NN, Haritos C, Vaxevanis CK, Anastasopoulou EA, et al. Differential intratumoral distributions of CD8 and CD163 immune cells as prognostic biomarkers in breast cancer. *J Immunother Cancer* 2017;5:39.
- [7] Pages F, Mlecnik B, Marliot F, Bindea G, Ou FS, Bifulco C, et al. International validation of the consensus Immunoscore for the classification of colon cancer: a prognostic and accuracy study. *Lancet* 2018;391(10135):2128–39.
- [8] Seo JS, Lee JW, Kim A, Shin JY, Jung YJ, Lee SB, et al. Whole Exome and Transcriptome Analyses Integrated with Microenvironmental Immune Signatures of Lung Squamous Cell Carcinoma. *Cancer Immunol Res* 2018;6(7):848–59.
- [9] Lee S, Margolin K. Tumor-infiltrating lymphocytes in melanoma. *Curr Oncol Rep* 2012;14(5):468–74.
- [10] Shalpour S, Karin M. Immunity, inflammation, and cancer: an eternal fight between good and evil. *J Clin Invest* 2015;125(9):3347–55.
- [11] Cavalleri T, Bianchi P, Basso G, Celesti G, Grizzi F, Bossi P, et al. Combined low densities of Foxp3(+) and CD3(+) tumor-infiltrating lymphocytes identify stage II colorectal cancer at high risk of progression. *Cancer Immunol Res* 2019;7(5):751–8.
- [12] Gabrielson A, Wu Y, Wang H, Jiang J, Kallakury B, Gatalica Z, et al. Intratumoral CD3 and CD8 T-cell densities associated with relapse-free survival in HCC. *Cancer Immunol Res* 2016;4(5):419–30.
- [13] Hu G, Wang S. Tumor-infiltrating CD45RO(+) Memory T lymphocytes predict favorable clinical outcome in solid tumors. *Sci Rep* 2017;7(1):10376.
- [14] Koelzer VH, Lugli A, Dawson H, Hadrich M, Berger MD, Borner M, et al. CD8/CD45RO T-cell infiltration in endoscopic biopsies of colorectal cancer predicts nodal metastasis and survival. *J Transl Med* 2014;12:81.
- [15] Yu X, Zhang Z, Wang Z, Wu P, Qiu F, Huang J. Prognostic and predictive value of tumor-infiltrating lymphocytes in breast cancer: a systematic review and meta-analysis. *Clin Transl Oncol* 2016;18(5):497–506.
- [16] Rusakiewicz S, Semeraro M, Sarabi M, Desbois M, Locher C, Mendez R, et al. Immune infiltrates are prognostic factors in localized gastrointestinal stromal tumors. *Cancer Res* 2013;73(12):3499–510.
- [17] Vitiello GA, Bowler TG, Liu M, Medina BD, Zhang JQ, Param NJ, et al. Differential immune profiles distinguish the mutational subtypes of gastrointestinal stromal tumor. *J Clin Invest* 2019;129(5):1863–77.
- [18] Balachandran VP, Cavnar MJ, Zeng S, Bamboat ZM, Ocun LM, Obaid H, et al. Imatinib potentiates antitumor T cell responses in gastrointestinal stromal tumor through the inhibition of IdO. *Nat Med* 2011;17(9):1094–100.
- [19] Casali PG, Abecassis N, Aro HT, Bauer S, Biagini R, Bielack S, et al. Gastrointestinal stromal tumours: ESMO-EURACAN clinical practice guidelines for diagnosis, treatment and follow-up. *Ann Oncol* 2018;29(Suppl 4):iv68–78.
- [20] Wei ZW, Xia GK, Wu Y, Chen W, Xiang Z, Schwarz RE, et al. CXCL1 promotes tumor growth through VEGF pathway activation and is associated with inferior survival in gastric cancer. *Cancer Lett* 2015;359(2):335–43.
- [21] Mijsch RC, Hao J, Schoenberg MB, Dotzer K, Schluter F, Weniger M, et al. Development of a reliable and accurate algorithm to quantify the tumor immune stroma (QTI_S) across tumor types. *Oncotarget* 2017;8(70):114935–44.
- [22] Hothorn T. Maxstat: maximally selected rank statistics. R package version 0.7-12; URL <http://CRAN.R-project.org/package=maxstat>.
- [23] Goeman JJ. L1 penalized estimation in the Cox proportional hazards model. *Biom J* 2010;52(1):70–84.
- [24] Wei JH, Haddad A, Wu KJ, Zhao HW, Kapur P, Zhang ZL, et al. A CpG-methylation-based assay to predict survival in clear cell renal cell carcinoma. *Nat Commun* 2015;6:8699.
- [25] Friedman J, Hastie T, Tibshirani R. Regularization paths for generalized linear models via coordinate descent. *J Stat Softw* 2010;33(1):1–22.
- [26] Harrell Jr FE. rms: regression modeling strategies. R package version 2016;5(2). URL <https://cran.r-project.org/web/packages/rms/>.
- [27] Seifert AM, Zeng S, Zhang JQ, Kim TS, Cohen NA, Beckman MJ, et al. PD-1/PD-L1 blockade enhances T-cell activity and antitumor efficacy of Imatinib in gastrointestinal stromal tumors. *Clin Cancer Res* 2017;23(2):454–65.
- [28] Binnewies M, Roberts EW, Kersten K, Chan V, Fearon DF, Merad M, et al. Understanding the tumor immune microenvironment (TIME) for effective therapy. *Nat Med* 2018;24(5):541–50.
- [29] Luen SJ, Salgado R, Fox S, Savas P, Eng-Wong J, Clark E, et al. Tumor-infiltrating lymphocytes in advanced HER2-positive breast cancer treated with pertuzumab or placebo in addition to trastuzumab and docetaxel: a retrospective analysis of the CLEOPATRA study. *Lancet Oncol* 2017;18(1):52–62.
- [30] Park JH, Jonas SF, Bataillon G, Criscitiello C, Salgado R, Loi S, et al. Prognostic value of tumor-infiltrating lymphocytes in patients with early-stage triple-negative breast cancers (TNBC) who did not receive adjuvant chemotherapy. *Ann Oncol* 2019;30(12):1941–9.
- [31] Toss MS, Miligy I, Al-Kawaz A, Alsleem M, Khout H, Rida PC, et al. Prognostic significance of tumor-infiltrating lymphocytes in ductal carcinoma in situ of the breast. *Mod Pathol* 2018;31(8):1226–36.
- [32] Zhou C, Diao P, Wu Y, Wei Z, Jiang L, Zhang W, et al. Development and validation of a seven-immune-feature-based prognostic score for oral squamous cell carcinoma after curative resection. *Int J Cancer* 2020;146(4):1152–63.
- [33] Savas P, Salgado R, Denkert C, Sotiriou C, Darcy PK, Smyth MJ, et al. Clinical relevance of host immunity in breast cancer: from TILs to the clinic. *Nat Rev Clin Oncol* 2016;13(4):228–41.
- [34] Nowicki TS, Akiyama R, Huang RR, Shintaku IP, Wang X, Tumeq PC, et al. Infiltration of CD8 T Cells and expression of PD-1 and PD-L1 in synovial sarcoma. *Cancer Immunol Res* 2017;5(2):118–26.
- [35] Jiang Y, Xie J, Han Z, Liu W, Xi S, Huang L, et al. Immunomarker support vector machine classifier for prediction of gastric cancer survival and adjuvant chemotherapeutic benefit. *Clin Cancer Res* 2018;24(22):5574–84.
- [36] Yu A, Mansure JJ, Solanki S, Siemens DR, Koti M, Dias ABT, et al. Presence of lymphocytic infiltrate cytotoxic T lymphocyte CD3+, CD8+, and immunoscore as prognostic marker in patients after radical cystectomy. *PLoS ONE* 2018;13(10):e0205746.
- [37] Turksma AW, Coupe VM, Shamier MC, Lam KL, de Weger VA, Belien JA, et al. Extent and location of tumor-infiltrating lymphocytes in microsatellite-stable colon cancer predict outcome to adjuvant active specific immunotherapy. *Clin Cancer Res* 2016;22(2):346–56.
- [38] Kovacs A, Stenmark Tullberg A, Werner Ronnerman E, Holmberg E, Hartman L, Sjostrom M, et al. Effect of radiotherapy after breast-conserving surgery depending on the presence of tumor-infiltrating lymphocytes: a long-term follow-up of the SweBCG91RT randomized trial. *J Clin Oncol* 2019;37(14):1179–87.
- [39] Kilvaer TK, Paulsen EE, Khanekkenari MR, Al-Saad S, Johansen RM, Al-Shibli K, et al. The presence of intraepithelial CD45RO+ cells in resected lymph nodes with metastases from NSCLC patients is an independent predictor of disease-specific survival. *Br J Cancer* 2016;114(10):1145–51.
- [40] Yajima R, Yajima T, Yanagita Y, Fujisawa T, Miyamoto T, et al. Tumor-infiltrating CD45RO(+) memory cells are associated with a favorable prognosis breast cancer. *Breast Cancer* 2016;23(4):668–74.
- [41] Iams WT, Shiuan E, Meador CB, Roth M, Bordeaux J, Vaupel C, et al. Improved prognosis and increased tumor-infiltrating lymphocytes in patients who have SCLC with neurologic paraneoplastic syndromes. *J Thorac Oncol* 2019;14(11):1970–81.
- [42] Seo AN, Lee HJ, Kim EJ, Kim HJ, Jang MH, Lee HE, et al. Tumor-infiltrating CD8+ lymphocytes as an independent predictive factor for pathological complete response to primary systemic therapy in breast cancer. *Br J Cancer* 2013;109(10):2705–13.
- [43] Donadon M, Hudspeth K, Cimino M, Di Tommaso L, Preti M, Tentorio P, et al. Increased infiltration of natural killer and T cells in colorectal liver metastases improves patient overall survival. *J Gastrointest Surg* 2017;21(8):1226–36.
- [44] Cheminant M, Bruneau J, Malamut G, Sibon D, Guegan N, van Gils T, et al. NKp46 is a diagnostic biomarker and may be a therapeutic target in gastrointestinal T-cell lymphoproliferative diseases: a CELAC study. *Gut* 2019;68(8):1396–405.
- [45] Nielsen JS, Sahota RA, Milne K, Kost SE, Nesslinger NJ, Watson PH, et al. CD20+ tumor-infiltrating lymphocytes have an atypical CD27- memory phenotype and together with CD8+ T cells promote favorable prognosis in ovarian cancer. *Clin Cancer Res* 2012;18(12):3281–92.
- [46] Shi WK, Zhang XH, Zhang J, Yu M, Yuan YJ, Xiong W, et al. Predictive ability of prognostic nutritional index in surgically resected gastrointestinal stromal tumors: a propensity score matching analysis. *Jpn J Clin Oncol* 2019;49(9):823–31.
- [47] Racz JM, Cleghorn MC, Jimenez MC, Atenafu EG, Jackson TD, Okrainec A, et al. Predictive ability of blood neutrophil-to-lymphocyte and platelet-to-lymphocyte ratios in gastrointestinal stromal tumors. *Ann Surg Oncol* 2015;22(7):2343–50.
- [48] Goh BK, Chok AY, Allen Jr JC, Quek R, Teo MC, Chow PK, et al. Blood neutrophil-to-lymphocyte and platelet-to-lymphocyte ratios are independent prognostic factors for surgically resected gastrointestinal stromal tumors. *Surgery* 2016;159(4):1146–56.
- [49] Guillerey C, Ferrari de Andrade L, Vuckovic S, Miles K, Ngwi SF, Yong MC, et al. Immunosurveillance and therapy of multiple myeloma are CD226 dependent. *J Clin Invest* 2015;125(5):2077–89.
- [50] Fridman WH, Zitvogel L, Sautes-Fridman C, Kroemer G. The immune contexture in cancer prognosis and treatment. *Nat Rev Clin Oncol* 2017;14(12):717–34.
- [51] Asano Y, Kashiwagi S, Goto W, Kurata K, Noda S, Takashima T, et al. Tumor-infiltrating CD8 to FOXP3 lymphocyte ratio in predicting treatment responses to neoadjuvant chemotherapy of aggressive breast cancer. *Br J Surg* 2016;103(7):845–54.
- [52] Aghdassi A, Christoph A, Dombrowski F, Doring P, Barth C, Christoph J, et al. Gastrointestinal stromal tumors: clinical symptoms, location, metastasis formation, and associated malignancies in a single center retrospective study. *Dig Dis* 2018;36(5):337–45.
- [53] Joensuu H, Vehtari A, Riihimäki J, Nishida T, Steigen SE, Brabec P, et al. Risk of recurrence of gastrointestinal stromal tumor after surgery: an analysis of pooled population-based cohorts. *Lancet Oncol* 2012;13(3):265–74.
- [54] Kuang DM, Zhao Q, Wu Y, Peng C, Wang J, Xu Z, et al. Peritumoral neutrophils link inflammatory response to disease progression by fostering angiogenesis in hepatocellular carcinoma. *J Hepatol* 2011;54(5):948–55.
- [55] Schrage Y, Hartgrink H, Smith M, Fiore M, Rutkowski P, Tzanis D, et al. Surgical management of metastatic gastrointestinal stromal tumour. *Eur J Surg Oncol* 2018;44(9):1295–300.
- [56] Borg C, Terme M, Taïeb J, Ménard C, Flament C, Robert C, et al. Novel mode of action of c-kit tyrosine kinase inhibitors leading to NK cell-dependent antitumor effects. *J Clin Invest* 2004;114(3):379–88.